Journal of proteome research reviews

New Developments in Profiling and Imaging of Proteins from Tissue Sections by MALDI Mass Spectrometry

Pierre Chaurand,[†] Jeremy L. Norris,[‡] D. Shannon Cornett,[†] James A. Mobley,[§] and Richard M. Caprioli*[,†]

Mass Spectrometry Research Center and Department of Biochemistry, Vanderbilt University Medical Center, Nashville Tennessee 37232-8575, Protein Discovery, Inc., Knoxville, Tennessee 37902, and Department of Urology, University of Alabama at Birmingham, Birmingham, Alabama 35294

Received July 12, 2006

Molecular imaging of tissue by MALDI mass spectrometry is a powerful tool for visualizing the spatial distribution of constituent analytes with high molecular specificity. Although the technique is relatively young, it has already contributed to the understanding of many diverse areas of human health. In recent years, a great many advances in the practice of imaging mass spectrometry have taken place, making the technique more sensitive, robust, and ultimately useful. The purpose of this review is to highlight some of the more recent technological advances that have improved the efficiency of imaging mass spectrometry for clinical applications. Advances in the way MALDI mass spectrometry is integrated with histology, improved methods for automation, and better tools for data analysis are outlined in this review. Refined top-down strategies for the identification and validation of candidate biomarkers found in tissue sections are discussed. A clinical example highlighting the application of these methods to a cohort of clinical samples is described.

Keywords: mass spectrometry • MALDI • tissue • proteins • profiling • imaging

Introduction

Mass spectrometry is rapidly becoming an analytical tool of choice to probe the molecular composition of tissue sections.[1−6] In this regard, matrix-assisted laser desorption ionization coupled with time-of-flight mass spectrometry (MALDI-TOF−MS) is an ideal method to obtain molecular profiles and images from thin frozen tissue sections in a high-throughput manner.[7,8] A protein profile can be obtained from any coordinate of a section by simple matrix deposition and its subsequent interrogation by MALDI−MS. When matrix is applied to the sections, after analysis, typically 300 and, in some cases, up to 1000 distinct mass signals can be observed in a mass-to-charge (m/z) range exceeding 200 000.[9] However, in many cases, it is the signals observed between m/z 2000 and 30 000 that are of the greatest interest. This is due to the interesting nature of the low molecular weight class of signaling molecules including chemokines, cytokines, and growth factors. To date, a number of studies have shown that signals observed in these profiles are tissue- and cell-specific. In general, the most intense signals come from the most abundant protein species. A precise limit of detection for the technology is, however, hard to estimate. This is due to a combination of factors such as the presence of ion-suppressing components which differentially attenuate ionization on a protein-to-protein basis. This point brings to light another issue regarding the relative quantification of peptide and protein peaks within any one tissue. This is an important point that will be addressed here in terms of data analysis and normalization, in addition to endpoints related to protein identification and clinical validation.

While the profiling of a tissue extract or nonspecific region on a tissue section can be of interest, especially in the case of more homogeneous sections, an imaging experiment becomes necessary when the focus is high-resolution protein distribution information within a tissue (Figure 1). For example, to better study tumor biology, the analysis of various cell types can be correlated to the tissues architecture, thereby allowing a mapping of differentially expressed peptides and proteins specific to the tumor and/or adjacent stroma. Therefore, high-resolution images are desirable when a defined substructure is present; however, they may also be utilized as a discovery tool for a suspected, yet otherwise nonvisually detectable, transformation such as has been observed for tumor margins in our laboratory. In the imaging experiment, an important aspect of sample preparation focuses on the homogeneous deposition of MALDI matrix in such a way as to avoid significant lateral migration of proteins on the surface of the section. To carry out this task in a reproducible manner, the MALDI matrix can either be deposited as high-density arrays of droplets[10] or in a homogeneous layer (coated) on the tissue section (depending on the spatial resolution required for the analysis) (Figure 1).[11] The mass spectrometric data is then acquired utilizing a grid pattern with a predetermined number

* Corresponding author: Richard Caprioli, Mass Spectrometry Research Center, 9160 MRB III, Vanderbilt University, Nashville TN, 37232-8575. Tel: (+1) 615 343 9207. Fax: (+1) 615 343 8372. E-mail: r.caprioli@vanderbilt.edu.
[†] Vanderbilt University Medical Center.
[‡] Protein Discovery, Inc.
[§] University of Alabama at Birmingham.

10.1021/pr060346u CCC: $33.50

Published on Web 10/04/2006

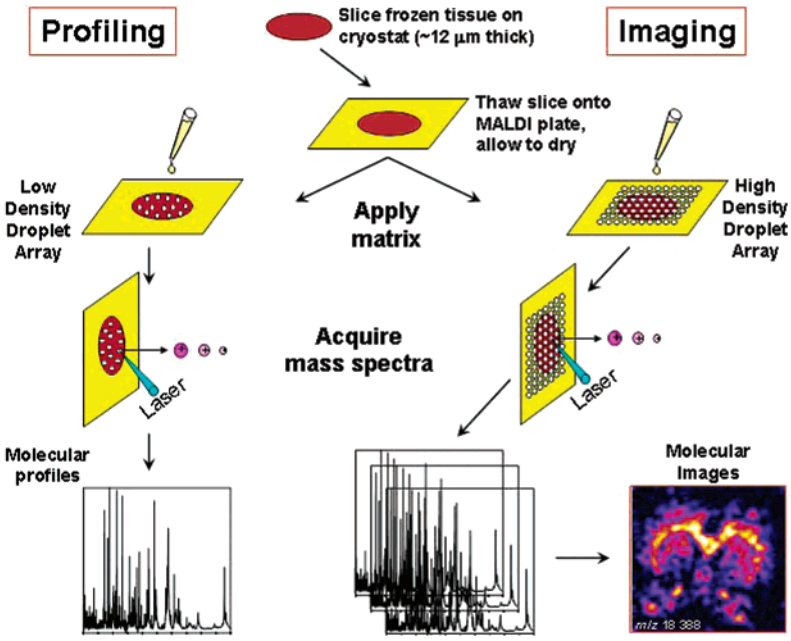

Figure 1. Scheme presenting the protein profiling and imaging analytical strategies from thin tissue sections.

of laser shots per grid coordinate. This pattern has a fixed center-to-center distance between spots, typically, 50 to 300 μm depending on the dimensions of the section and the imaging resolution required. Data acquisition and processing are carried out with specialized algorithms.[12,13] The second step in data processing involves image reconstruction and the integration of preprocessed signal intensities for desired m/z values, for each pixel, across the entire dataset. From this perspective, a single imaging experiment will generate literally hundreds of individual protein density maps or images. Incorporation of on-the-fly statistical analysis is necessary to allow one to make full use of this type of multivariate data.

The potential for this type of analysis, in which the spatial distribution of specific molecular species are mapped throughout a tissue section, is particularly exciting for the study of elusive processes involving disease initiation and progression.[14,15] While this capability is routinely available for known individual proteins via immunohistochemistry, IMS offers the potential for the simultaneous analysis of many molecular species present in a single tumor regardless of the availability of specific antibodies. In addition, this technology has the added benefit of imaging the tissue distribution of low molecular weight (MW) compounds such as drugs and metabolites,[16−18] thereby opening new possibilities for the measurement of concomitant protein changes in specific tissues after systemic drug administration.[19,20] In combination with rapid advances in informatics, IMS offers the capacity for an entirely new and highly precise means of analyzing diseased tissue. In a broader context, with continued advances in instrumentation speed, and data processing, in addition to an increased understanding of molecular pathogenesis, it will be possible to acquire proteomic profiles for a tumor section within a time frame that is not far outside what is expected for a detailed histologic examination.[15] This information could significantly impact the course of therapy for a particular tumor and would be available before the patient leaves the operating room.

Over the past 5 years, numerous improvements to IMS of peptides and proteins have been made by various groups, including our own laboratory, which revolve around (1) sample preparation methodologies,[10,11,21−24] (2) instrumentation,[25−29] and (3) algorithms for data acquisition and processing.[12,13,30,31] Here, we review the protocols and methodologies that we routinely employ to profile and image peptides and proteins in thin tissue sections by MALDI−MS. We also describe some of the data processing tools necessary to explore the information recovered in these profiles and images to the fullest extent, in addition to some of the latest perspectives on protein identification for the downstream clinical validation of biomarkers.

Tissue Handling and Processing

To date, in our laboratory, only sections from fresh frozen tissue blocks have been utilized for MALDI−MS analyses. In this case, no fixative agents containing protein cross-linkers are added, and for most tissues, the protein profiles recovered from the sections should reflect the original proteomic content when frozen immediately after sampling to minimize protein degradation. Tissue biopsies or other relevant tissue samples should therefore be frozen immediately after acquisition in liquid nitrogen or isopentane in order to preserve the sample's morphology and minimize protein degradation through enzymatic proteolysis. Tissue orientation and morphology are best preserved when the biopsies are loosely wrapped in aluminum foil. Specimen cassettes or plastic tubes should therefore be avoided. Some samples, such as mouse brain or, in general, bigger specimens, may shatter when rapidly plunged in liquid nitrogen. To avoid shattering, it is therefore recommended to slowly plunge the sample in the freezing liquid. Once frozen, the specimens may be kept at −80 °C for extended periods of time without major sample degradation.

For most applications, 5−20 μm thick sections are cut at −15 °C (exact cutting temperature is tissue-dependent) and thaw-mounted on an electrically conductive flat sample plate. To maintain the specimen to be cut in position on the cryostat head, it is typically held in place using embedding medium (Figure 2a). At this point, orientation is critical and should be considered. Total immersion of the specimen-embedding

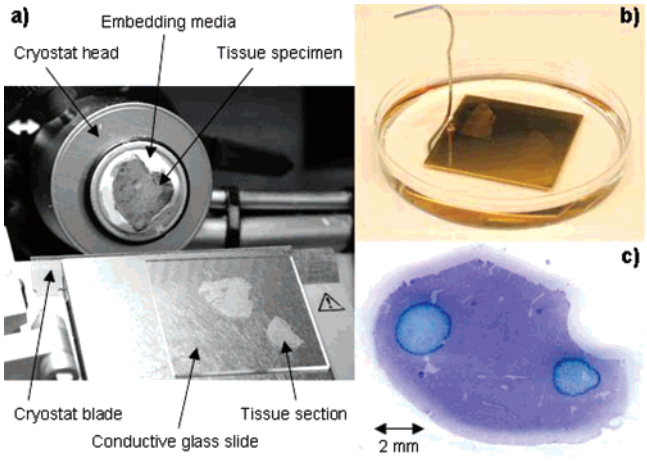

Figure 2. Tissue specimen processing toward MALDI−MS analysis. (a) The tissue block is oriented and maintained in position on the cryostat head in order to be cut in thin (~12 μm) sections. The sections are then thaw-mounted on conductive glass or metallic target plates. (b) The sections are then rinsed in a graded ethanol series prior to matrix deposition. (c) Sections can be stained with cresyl violet prior to matrix deposition. In this example, matrix (sinapinic acid) was subsequently deposited by hand forming spots ~2 mm in diameter. See text for more details.

medium should be avoided. We have found that when the cryostat blade first touches the embedding medium, a thin film of medium contaminates the section which leads to poorer quality data.[11] Most disposable cryostat blades are often packaged with a very thin film of oil between each blade. To avoid contamination from this oil, it is recommended to rinse the blades with methanol and acetone prior to sectioning. In our laboratory, tissue sections varying in thickness between 5 and 20 μm have been successfully analyzed. Within this thickness range, minimal spectral variations have been observed when the sections were manually spotted with matrix. When matrix is deposited on the sections by a spray approach (see below), thickness has however been found to be critical.[32] Best results were obtained for thicknesses ranging from 2 to 10 μm. The thickness may however be of importance if the section is to be stained after the MS analysis (see below). In this case, thinner sections are preferred, allowing better observation of histological features. After the section is cut, it needs to be thaw-mounted on the MALDI sample plate (Figure 2a). To do so, the best approach is to drag and lay out the section, with a small paintbrush, on the plate (maintained cold in the cryostat chamber) with the desired orientation. Once the section (at this point still frozen) is in position, it is thaw-mounted by warming the bottom of the sample plate on one's hand within the cryostat chamber. Macroscopic drying of the section usually takes 20−30 s. Once the section is dried, the now warm plate can be removed from the cryostat housing without condensation of atmospheric water. If multiple sections are to be mounted, the slide should be kept in the cryostat housing and must be cold (below freezing) in order to mount additional sections. Completely drying each section avoids repeated freeze−thaw events, therefore, virtually eliminating occurrence of "freezer burn" marks that make the sections brittle and prone to detachment from the target surface. After sectioning, sections are further dehydrated in a desiccator for several minutes prior to MALDI matrix deposition.

At this point, the MALDI matrix can be deposited on the sections. We have, however, found that rinsing (fixing) the sections prior to matrix deposition significantly enhances the quality of the MS data.[10,21,33] After fixing, overall ion yields augment by a factor of at least 3-fold and, in some cases, up to 10-fold. The fold increase depends on the type of tissue investigated. The following procedure has been optimized and tested on numerous types of different tissues and has proven particularly helpful for the analysis of proteins. Sections (on the target plates) are first fixed in a 70% ethanol (HPLC-grade) solution for 30 s. This can be done in a Petri dish by fully immersing the target plate and gently stirring the ethanol solution (Figure 2b). This first step is followed by a second fixation step in a mixture of 90% ethanol, 9% glacial acetic acid, and 1% deionized water for 30 s. After rinsing, the sections are allowed to fully dry in a vacuum desiccator for several minutes. We have found that this rinsing procedure eliminates physiological salts and most phospholipids from the sections. Also, ethanol is a known protein fixative, precipitating the proteins *in situ*, therefore, minimizing protein solubilization and delocalization from the sections. Fixed sections are also more stable over time and, in most instances, can be kept for several days (up to seven) in a desiccator before they are analyzed.

For some tissue specimens (i.e., unusual shape or size), the use of embedding media is inevitable to successfully cut sections. In this case, some embedding media will be collected on the target plates around the thaw-mounted sections. Most embedding media are highly soluble in water, and a section-rinsing procedure has been optimized to remove it in large part. First, sections undergo the same rinsing protocol as mentioned above in 70% and 90% ethanol-based solutions for them to adhere to the target plate. The sections are then brought back down to 70% ethanol for 30 s followed by 30 s in deionized water. This step was found to be very helpful in removing remaining embedding media without removing the sections from the target plates. Sections are then rinsed again in 70% and 90% ethanol-based solutions. Good quality protein profiles can be generated after embedding, showing no significant loss of protein signals with respect to matching nonembedded specimens.

Historically, tissue sections have been thaw-mounted on flat metallic target plates such as aluminum, stainless steel, and gold-coated plates. Gold-coated target plates generally offer a fairly nice contrast, which usually allows visualizing major histological features of the sections. Further, sections usually "stick" well to gold-coated targets, especially during the rinsing procedures. However, with opaque target plates, little to no microscopic visualization of the section is possible. We have recently begun using conductive glass slides as a target plate[21] (Figure 2a). These slides (Delta-Technologies, Stillwater, MN) are coated with a very thin (~130 Å) film of indium−tin oxide, rendering them electrically conductive and allowing uniform maintenance of the high voltage potential in the ion source of MALDI-TOF mass spectrometers. Such conductive slides have been found to be stable for all MALDI-TOF−MS applications, providing high-quality data under delayed extraction conditions with laser repetition rates of up to 200 Hz. Since these glass slides are transparent, observation of the sections by light microscopy is now possible. In parallel to the use of glass target plates, we have tested for the compatibility of several tissue section staining protocols with MALDI−MS.[21] We found that several nuclear dyes offered good staining qualities without interfering with the MALDI process (Figure 2c). Ultimately,

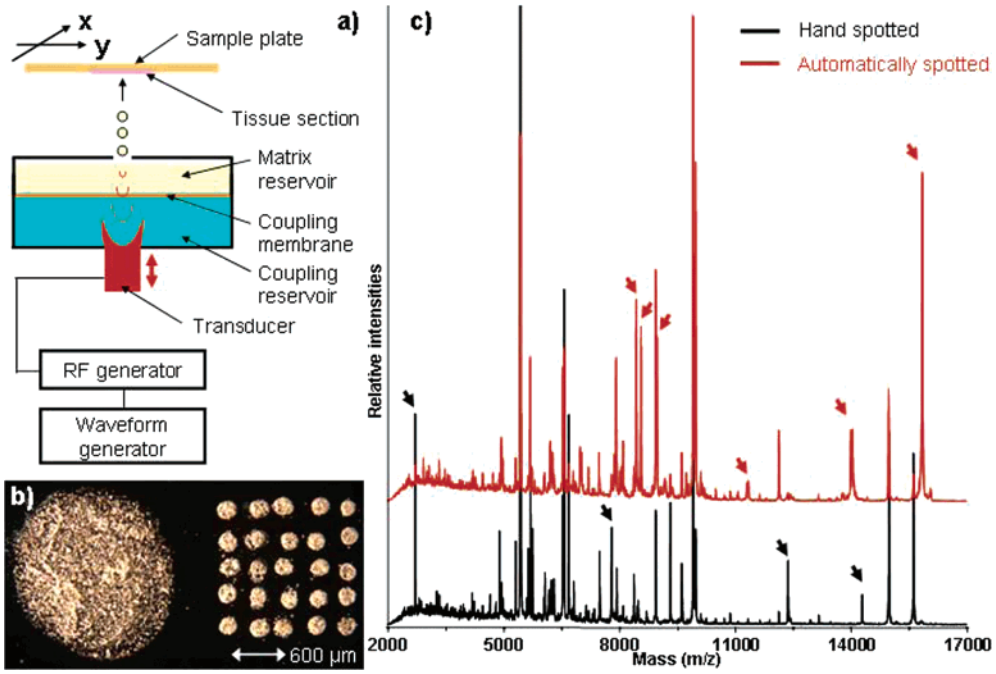

Figure 3. Comparison between hand and automated matrix deposition on tissue sections. (a) Schematic representation of the acoustic droplet ejection robot. Matrix droplets are vertically ejected from an opened face reservoir under the action of a sound wave generated by a vibrating transducer. (b) The accumulations of tens of drops of matrix (sinapinic acid) form very small spots ~200 μm in diameter on tissue sections in comparison to the drop formed by hand deposition (300 μL, twice). (c) MALDI-TOF−MS protein profiles obtained from the analysis of hand and automatically spotted sinapinic acid on a mouse liver section. See text for more details.

staining with cresyl violet offered the best combination of staining contrast and MALDI−MS performance. This staining protocol allows us to visualize the histological features on the sections to be analyzed allowing a more accurate matrix deposition.

Section staining can also be performed after MALDI−MS analyses.[30] Coloring sections with hematoxylin and eosin (H&E) is a typical staining protocol widely used in most pathology laboratories. Prior to H&E staining, the matrix needs to be removed from the surface of the sections. To do this, the sections are plunged for about 1 min in a 70% ethanol solution while gently stirring the target plate. Most matrixes, sinapinic acid in particular (see below), are highly soluble in water−ethanol mixtures. Once the matrix is removed, further dehydration of the section in graded ethanol series can continue toward H&E staining.

Matrix Deposition and Mass Spectrometry

The MALDI mass spectra presented here were generated either on an Applied Biosystems (Framingham, MA) Voyager DE-STR or a Bruker Daltonics (Billerica, MA) Autoflex II time-of-flight mass spectrometer. MS data were acquired in the linear mode with an accelerating potential of 20 kV under optimized delayed extraction conditions. The Voyager DE-STR is equipped with a 337 nm N_2 laser operating at a repetition rate of 20 Hz, while the Autoflex II is equipped with a solid-state SmartBeam laser operating at adjustable repetition rates up to 200 Hz.[34] MS Images were acquired with the Autoflex II using a new protocol[35] whereby matrix spots are transformed into sample wells of a custom plate geometry. Spectra were acquired from each spot using the AutoXecute function and subsequently converted into a format compatible with the image viewer software, BioMap (Novartis, Switzerland).[13]

For protein profiling and imaging purposes, the MALDI matrix can either be deposited as individual droplets (spotted) or as a homogeneous layer (coated) on the tissue section, depending on the spatial resolution required for the analysis (Figure 1). In our hands, the matrix of choice for protein analyses has been found to be sinapinic acid. For manual matrix deposition, sinapinic acid is typically prepared at 20 mg/mL in a mixture of 50% acetonitrile, 50% deionized water, and 0.1% trifluoroacetic acid. In this case, droplets as small as 200 nL can be deposited onto the sections using an automatic pipet. Sections are typically spotted twice to increase crystal density. Deposition of 200−300 nL of matrix solution typically leads to a spot size of about 2 mm in diameter (Figure 2c). If smaller matrix spots are required, matrix can also be manually deposited using a fine-pulled capillary under low magnification conditions. In this case, individual spots of 50−100 μm in diameter can be achieved. When the solvents have evaporated and MALDI crystals have formed, the samples are ready to be analyzed. Best results are obtained when the samples are promptly analyzed. However, spotted tissue sections can be kept overnight in a desiccator without major loss of signal. After hand-spotting of matrix on a tissue section, 300−500 distinct protein mass signals are observed in a MW range up to and, in some cases, exceeding 200 000.[9] However, over 90% of these signals are observed in the MW range from 2000 to 30 000 over 2 to 3 orders of magnitudes for the lower MW proteins (see Figure 3c).

MALDI matrix can also be deposited on a tissue section in an automated fashion. We have recently successfully tested matrix deposition via a robotic printer.[10] The matrix printer utilizes acoustic energy to generate very small droplets of matrix (~120 pL) on the tissue sections to generate a matrix spot. Figure 3a presents a schematic view of this printer (Acoustic Reagent Multispotter, Labcyte, Sunnyvale, CA) which has been

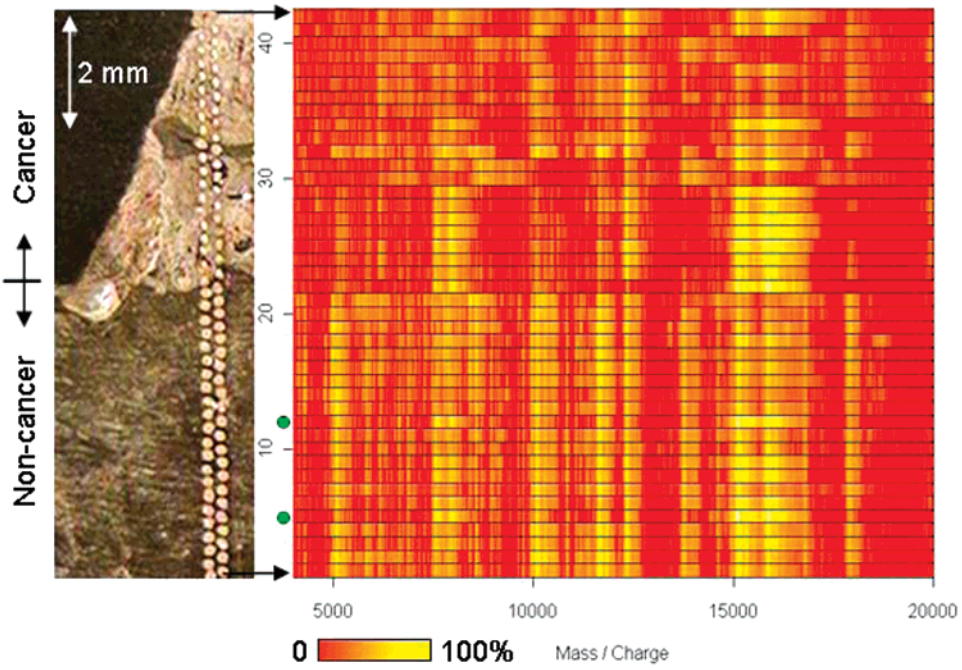

Figure 4. Protein profiles, displayed as a heat map, obtained upon MALDI−MS analysis of a 12 μm thick human renal cell carcinoma and surrounding nontumor tissue biopsy section after automated matrix deposition. Significant variations in protein signal expression were observed between the cancerous and noncancerous cells.

recently described in details elsewhere.[10] Briefly, matrix solution (sinapinic acid at 25 mg/mL in the solvent system described above) is deposited in a 1.5 mL reservoir. This reservoir is constructed from an acoustically transparent membrane that is coupled to a piezo transponder by way of a column of water. The transponder vibrates at a given amplitude and frequency and is shaped such as to produce a sound wave focused at the surface of the matrix solution in the reservoir. When the sound wave reaches the surface, it vertically ejects droplets of matrix with a volume of approximately 120 pL. These droplets are then collected on the tissue section held inverted over the matrix reservoir. Since the droplets are ejected from a large surface reservoir, there is no possible clogging, which can be the case when using nozzles in piezo-type printers. Fifty to 70 droplets are typically collected to form a matrix spot with a diameter of ~200 μm. Figure 3b compares the matrix spot obtained after hand-depositing 300 nL of matrix twice with those obtained from the robotic printer. Within the surface of each microspot, about 500 individual laser shots can be fired producing good quality mass spectra before seeing significant loss of ion yield due to matrix ablation. Figure 3c compares the MALDI−MS protein profiles obtained by analyzing a 12 μm mouse liver section after hand or automated matrix deposition. In both cases, very similar profiles were recovered when considering the m/z species observed and their relative intensities. In the spotter, the target plate is positioned in a holder mounted on a precise two-dimension translational stage. When the stage is moved between each droplet ejection event, arrays of small spots can be printed in a Cartesian pattern over the entire surface of the sections. This approach limits protein delocalization to the tissue surface covered by the spot. Other matrix spotters are available, in particular, the CHIP chemical spotter from Shimadzu Biotech (Columbia, MD) (currently tested in our laboratory for matrix array deposition) and the TM iD platform from LEAP Technologies (Carrboro, NC).

Of particular interest from a clinical standpoint is the study of the changing molecular events that are found at the border of tumors and histologically classified normal tissues. Figure 4 presents the analysis by MALDI−MS of a human renal cell carcinoma biopsy that clearly presents tumor and adjacent noncancerous tissue. Droplets of matrix (sinapinic as matrix at 25 mg/mL in 50/50/0.1 of acetonitrile/H_2O/TFA) were deposited every 250 μm forming rows across the sections. For every droplet, the resulting spectrum was plotted as an intensity band in the m/z range from 4000 to 20 000. When all of the data points are combined, the resulting heat map clearly displays numerous signal intensity variations between the cancerous area (top of the section) and the adjacent noncancerous tissue (bottom of the section). Furthermore, significant differences were also observed within the cancerous area, an observation consistent with the heterogeneous cellular content of the tumor. Interestingly, several traces acquired from spots deposed on the noncancerous area (particularly traces 5 and 12, highlighted with green dots) present profiles with features consistent with those acquired from the cancer area (traces 22−29).

We have used this matrix-spotted array approach to "homogeneously coat" tissue sections to perform IMS measurements. In this case, each spot is interrogated and becomes a pixel for the resulting protein ion images. The center-to-center distance between each spot defines the imaging resolution. The time required for data acquisition depends on the area of the tissue to be analyzed, the resolution at which the matrix has been printed, and the laser repetition rate used. Figure 5 presents the IMS analysis of a xenograft grown from lung tumor cells in the hind limb of a nude mouse. For this analysis, tissue cutting and rinsing and matrix spotting, as well as data acquisition, were all performed within the same day. A section was cut at a thickness of 12 μm, rinsed following the protocol mentioned above, prior to printing a sinapinic acid matrix array

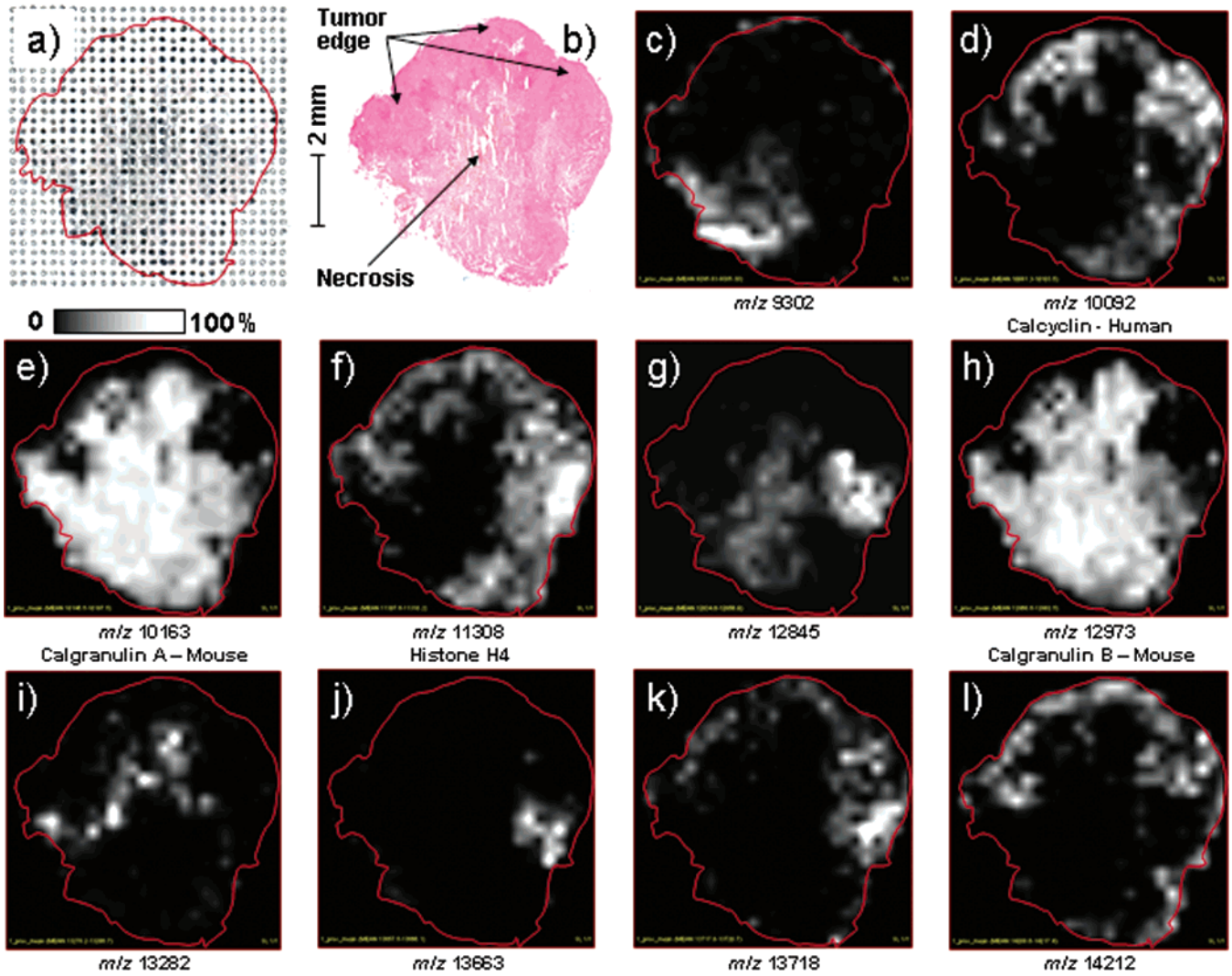

Figure 5. MALDI mass spectrometry imaging of a xenograft tumor grown from a lung cancer cell line. (a) Photomicrograph of a 12 μm thick section after automatic deposition of a 28 $\times$ 28 matrix droplet array with a center-to-center distance of 300 μm between spots. (b) H&E-stained serial section clearly showing areas of living cancer cells on the edge of the tumor, as well as a necrotic center essentially composed of dead cells. (c–l) Ion density maps obtained for proteins of different *m*/*z* values, some of which have been previously identified. Some proteins are preferentially expressed along the tumor edge, while others are most abundant within the necrotic center.

with a 300 μm distance between spots. Figure 5a shows a photomicrograph of the investigated section after matrix deposition. A spot array consisting of 28 rows and 28 columns (784 spots) has been printed using sinapinic as matrix. Figure 5b presents a photomicrograph of an H&E-stained serial section. Particularly noticeable from this section are areas of living cancer cells visible on the borders of the tumor, while the center is essentially composed of dying or dead cells (necrotic area). Figure 5c–l presents 10 ion density maps for proteins of different MW. These images clearly show that some proteins are only localized within the growing edge of the section (*m*/*z* 10 092, 11 308, and 14 202), while others are highly expressed within the necrotic areas (*m*/*z* 10 163 and 12 973). Other proteins were found to be abundant in other parts of the xenograft. Of particular interest is the protein at *m*/*z* 13 282, which is expressed at the interface between the living cellular edge and the necrotic area. The histology of this portion of the section revealed a high abundance of dying cells.

Other matrix deposition techniques for homogeneous deposition have been developed. The first reported approach consists of dragging a large drop of matrix over the section.[7] About 50–100 μL of matrix are deposited next to the section to be analyzed. This large drop is then dragged and spread over the surface of the section in one homogeneous motion and allowed to dry. Best results are obtained when this operation is performed at 4 °C in a cold room. Although this approach generally gives good quality spectra, the risk of delocalizing proteins during the coating process is very high. Further, crystal coverage on the section is low, in the order of 50%. In our hands, after matrix coating using the large drop approach and subsequent IMS measurements, about 1 in 5 sections gave good quality images. Nevertheless this matrix coating approach is still used by others with some success associated with matrix pre-seeding,[13,31,36] and particularly with the recent development of ionic matrixes for IMS.[24]

A last matrix deposition approach is spray coating. If matrix is homogeneously deposited, then the factors limiting the imaging resolution are the MALDI crystal size and the dimension of the ionizing laser beam. In most commercially available MALDI-TOF mass spectrometers equipped with compact ni-

trogen lasers (337 nm), laser spot diameters in the order of 50 μm can be achieved on target with limited efforts. One approach is to collimate the laser beam using an adjustable iris.[7] One example of a scanning MALDI-TOF system with a beam profile of less than 1 μm on target obtained with a nitrogen laser has, however, been reported.[25] For instruments equipped with solid-state lasers, because the laser beam profiles are in this case much better defined, smaller spot sizes in the 10−25 μm range can be obtained.

Two approaches for spray deposition of matrix on tissue sections have been proposed, pneumatic and electrospray deposition. The first consists of a pneumatic-assisted spray deposition of matrix using a small handheld nebulizer, typically used to spay thin liquid chromatography plates.[9,11] The nebulizer is coupled with a nitrogen bottle used to propel the matrix solution. For the imaging of proteins, sinapinic acid is again preferred as matrix (25 mg/mL in 50/50/0.1 of acetonitrile/H_2O/TFA). Matrix pneumatic spray deposition is performed in cycles. The spray parameters need to be carefully controlled as not to "overwet" the section. Overwetting of the section typically leads to the delocalization of some proteins over the surface of the section resulting in poor image quality. A wet interface is, however, required to locally solubilize proteins from the section.[37] To homogeneously coat sections with a high crystal density, about 10 spray cycles are required. If too many spray cycles are overlaid, one runs the risk of depositing too much matrix forming multiple crystal layers, which eventually quench ion yield. Each spray cycle only lasts a few (5) seconds, depending on the area to be coated. Between each cycle, the section is allowed to dry for about 1 min. Progress in the coating process can be followed by observing the section under a microscope. Ultimately, a homogeneous monolayer of crystals of about 30 μm in dimension can be formed, covering over 90% of the surface of the section.[9] Along with the high risk of protein delocalization, another major drawback of matrix deposition via pneumatic spray coating is the poorer quality of the MS data.[9] When compared to protein profiles obtained after hand or automated drop deposition of matrix, the profiles obtained after spray deposition exhibit a significant loss of overall signal intensity and higher noise accompanied by a loss of resolution. This ultimately leads to a significant loss of the overall number of observed protein signals from the sections. Several IMS examples where spray coating was used for sample preparation for the study of local protein composition on tissue sections have nevertheless been successfully performed.[8,19,32,38,39] Automation of pneumatic matrix spray deposition is currently being developed by several groups (homemade systems). A commercially available matrix spray system exists from LEAP Technologies (Carrboro, NC).

With electrospray deposition of matrix, very controlled amounts of matrix can be deposited to form a homogeneous coating. The spray needle can be mounted on a motorized $X-Y$ stage to precisely control its parallel movement with respect to the tissue section. To obtain stable spay conditions, the matrix is dissolved in high percentage of organic solvents such as acetone. One of the major drawbacks of the electrospray approach is the limited amount of moisture that reaches the tissue section, limiting the local solubilization of peptides and proteins and the formation of MALDI crystals. Although this tissue coating approach is not used in our laboratory, it has been used by others. Success in spraying α-cyano-4-hydroxy cinnamic acid as matrix has been reported for the imaging of peptides.[40]

Biomarker Discovery and Clinical Applications

Profiling and imaging mass spectrometry have proven effective for the discovery and monitoring of disease-related proteins.[14,15,41] Previous examples include markers for the classification and prognosis of cancer of the brain[42−44] and lung,[45] as well as applications in toxicology[19,46] and understanding the mechanism of disease.[47−51] The cited examples demonstrate the powerful ways in which this technique can be applied; however, some practical steps must be taken to ensure that the data is suitable to address the problem of interest. Methods for proper sample preparation have been discussed that ensure some acceptable measure of reproducibility and robustness. The generated mass spectra undergo a series of processing steps to prepare the data for statistical analysis; the final result is a set of biomarker candidates that are ready for identification and validation. The process of generating and analyzing MALDI mass spectral profiles for the purpose of biomarker identification is demonstrated here using a small cohort of human breast cancer biopsies.

Histology-Directed MALDI Analysis of Breast Tumors. A total of 38 breast tumor biopsies containing invasive mammary carcinoma that were previously determined by immunohistochemistry to be clinically positive or negative for estrogen receptor alpha (ER-α) was analyzed using MALDI mass spectrometry. All of the tumors were sectioned at a thickness of 12 μm and thaw-mounted in a single experiment onto two separate MALDI target plates. Serial sections were also collected for each tissue and H&E-stained for use in the histology-directed matrix application.[61] For each sample, areas of interest were marked for application of matrix by matching features in the stained sections with those on the unstained serial sections. These areas were marked in the control software for the automated matrix spotter and stored for later deposition of matrix. The matrix was deposited in an automated fashion using the methodology mentioned above. Prior to MS analysis, each section was thoroughly screened by a pathologist to verify that the correct tissue locations were targeted for analysis. The spotted sections were then analyzed by MALDI−MS in an automated fashion, and mass spectra were collected by averaging signals from 750 laser pulses per matrix position. Selection criteria were set to prevent failed spectra from being saved.

Data Analysis Methods. The collected data were analyzed using a set of tools developed by industry partners and internally at Vanderbilt University. The workflow for data analysis applied in this study is shown in Figure 6. Baseline subtraction, noise estimation, and spectral realignment were performed using ProTS-Data software (Biodesix, Inc., Steamboat Springs, CO). The algorithms used to compute the baseline and noise estimation are based on local estimates of peak width. The peak width changes as m/z increases; therefore, local parameters are set to compute the most accurate baseline and noise.[52] The background signal contributed by chemical and instrument noise is subtracted from the spectra prior to performing any comparative analysis.

To ensure that spectral comparisons are most accurate, the spectral features must be normalized to correct for variations in intensity and aligned to compensate for irregularities in m/z. Spectral normalization is performed by scaling the intensity of the spectrum according to a normalization factor. The origin of this normalization factor can vary, but one common way that is effective for the majority of situations is scaling according to the total measured ion current (TIC). In fact, in situations whereby very few peaks change among the groups that are

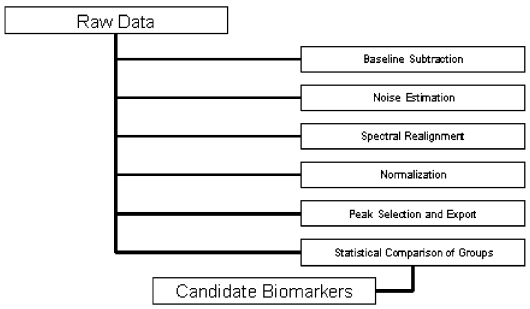

Figure 6. Mass spectra analysis work flow. The mass spectra are treated to processing algorithms responsible for the removal of noise, realignment of the *m*/*z* scale, and peak selection and matching. The data are returned to a table, formatted for statistical analysis using a number of established methods. The result of the analysis is a list of biomarker candidates that are subjected to further validation steps.

being compared, TIC can be used as a quite reliable normalization factor. In situations where greater than 10% of the spectral features are altered, one must be cautious in applying such an approach. In these cases, more sophisticated algorithms that estimate spectral intensity independent of the effect of ions unique to a single group have been developed.[53] Alignment of the spectra according to *m*/*z* is performed using routine algorithms and can also be used to further calibrate spectra based on a set of common peaks that may be utilized as landmarks. In this case, the data is screened prior to alignment to identify peaks that consistently appear in the data set. Ions that occur in greater than 90% of the measured spectra are selected and applied to the data set as calibration points. The assigned value for a chosen calibration point is the median value measured for that particular ion. Since the theoretical mass is not necessarily known for the alignment points, this cannot be considered a true calibration, that is, unless internal calibration standards are added to a few tissue sections in order to calculate the mass for common landmarks. However, with a properly calibrated instrument, the deviation away from the true *m*/*z* scale is generally minimal.

Having performed all of these preprocessing tasks, one is now prepared to export the necessary information to make a statistical analysis of the data. Although the data can be compared on the basis of the whole spectrum,[54] in this case, peak lists were exported and analyzed. The peaks were matched or binned using algorithms developed at Vanderbilt University. The exported ions are aligned across samples by use of a genetic algorithm parallel search strategy as previously described.[45] The peaks are binned together such that the number of peaks in a bin from different samples will be maximized, while the number of peaks in a bin from the same sample will be minimized. The results from binning yield a simplified data set that identifies only the regions of the spectrum that contain peak information. The *m*/*z* ranges defining peaks are used as boundaries to integrate the area under the curve for each peak and from each spectrum. A table is then constructed that lists the peak areas computed from each of the measurements made. The net result is that spectra containing greater than 50 000 individual data points are reduced to a matrix having fewer than 500 data points and containing only pertinent information. To further clarify a major point, newer developments address the challenge of reproducible peak picking (especially for low-intensity signals) by extracting signals from every spectra within a bin range where a "real" peak is measured (i.e., signal-to-noise > 3) in any one spectra. This circumvents a common error in underrepresented regions that would otherwise be assigned a value of zero simply because a peak was not detected.

Result: Novel Molecular Markers Correlate with a Patient's ER Status. The determination of ER-α status is an important predictive factor for response to endocrine therapy in breast cancer patients (i.e., tamoxifen). The purpose of this study is to develop an alternative screening tool for characterizing these patient groups. Once the data is reduced as described above, a number of statistical tests can be performed. In this case, the candidate peaks were ranked according to the significance of the change using a weighting factor accounting for mean and standard deviation of the normalized intensity.[46,54,55] Seven ions were found to have changed in a statistically significant manner when comparing the two patient groups. The top weighted markers were ranked accordingly, three of which are displayed in Figure 7. The molecular changes that correlate with ER-α status will be subjected to further study in terms of protein isolation and characterization, in addition to validation using classic immunohistochemistry-based studies and/or newer bottom-up quantitative approaches using heavy-labeled synthetic peptides.[56]

Strategies for the Rapid Isolation and Identification of Biomarkers

The identification of molecular markers observed in MALDI−MS profiles and images presents a unique set of challenges that is beyond the scope of this review; however, we attempt to highlight here some of the more important aspects. From this perspective, while profiles generated from these types of studies are proving to be of great interest, there is equal interest in validating the more significant markers. After tissue profiling and imaging, the only information recovered is the precise MW values (~150 ppm accuracy) for the biomarkers to be identified. One important aspect is to assess to which type of ion species these signals correspond to. In MALDI−MS, ionization typically occurs by the capture of a single proton by the protein forming a singly charged molecular ion of the form $[M + H]^+$, where M is the MW of the protein. In this case, the MW of the protein can easily be determined. However, in some instances, proteins can also be detected in the doubly charged form $[M + 2H]^{2+}$. In other cases, ionization may also occur through cation transfer, forming salts of sodium $[M + Na]^+$ and potassium $[M + K]^+$, or even through matrix transfer forming matrix adducts. Ultimately, a careful examination of the profiles usually allows to assess which type of ion is observed and to derive an accurate molecular weight. In addition, the proteins can be, and often are, oxidized, truncated, post-translationally modified, or covalently bound to metals such as selenium, iron, or copper. All of these phenomena may have an incidence on the molecular signature observed in the mass profiles and the effective molecular weight of the proteins. Since the observed *m*/*z* value is the only link to a protein marker to be identified, the extraction and identification process must be carried out in a strict manner. A more positive note revolves around the fact that the proteins detected from a tissue profiling experiment tend to be of higher abundance and are therefore more amenable to identification.

Protein identification cannot be performed uniquely on its MW information because numerous proteins may have close or, in some cases, the same nominal mass. Therefore, one must establish either a true top-down or a top-down-directed

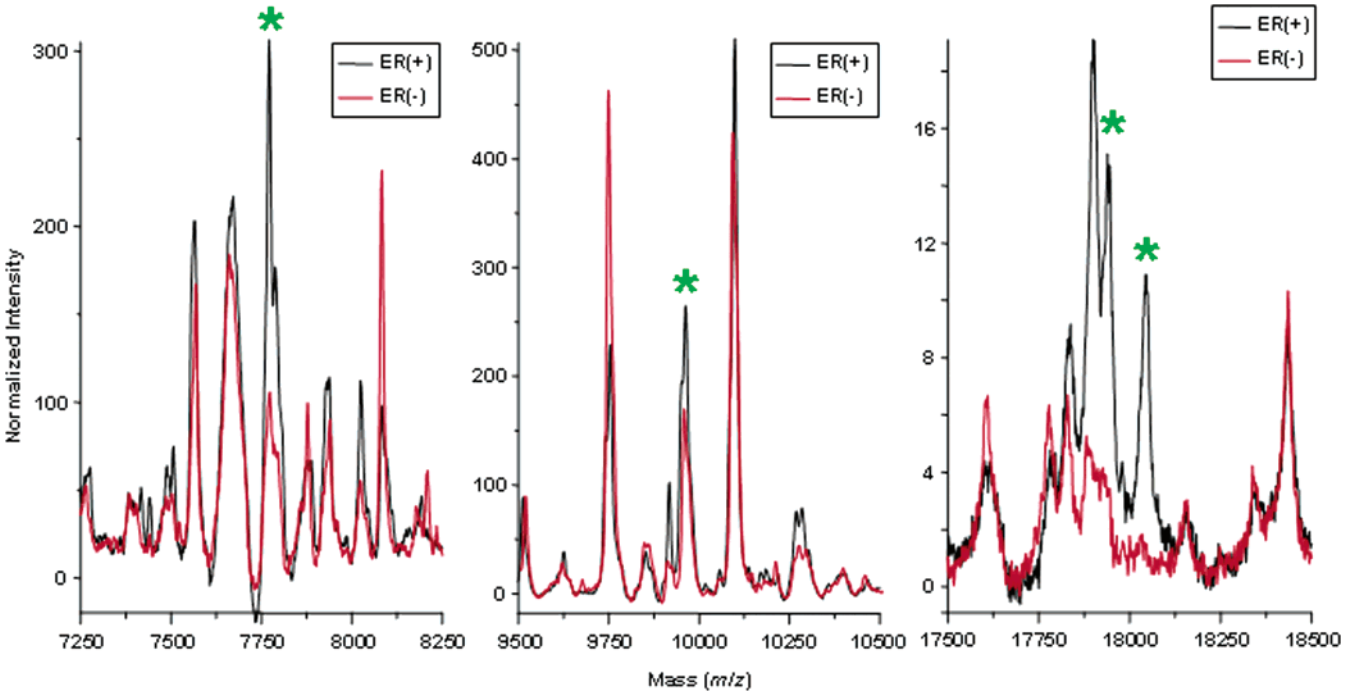

Figure 7. Partial average spectra are displayed for both the ER-positive and ER-negative patient group. Highlighted (asterisk) above are a set of candidate markers that were identified as changed when comparing the two groups. Ions of *m/z* 7760, 9979, 17 943, and 18 084 were found to be changed at statistically significant levels.

separation methodology as described in short here. While a true top-down approach carried out on tissue is most desirable, and has been described for low MW peptides on tissue,[46,57] we have found that it is extremely challenging to isolate and fragment a singly charged protein of appreciable mass directly from tissue, even with modern instrumentation such as MALDI FT-ICR and TOF/TOF instruments. In some cases, especially for lower MW proteins (<5000), generating partial fragmentation information was successful and found useful to verify the identity of previously identified proteins.

Protein identification typically begins with several sequencial isolation steps followed by protein characterization by tandem MS. The first step consists of extracting proteins using whole protein extraction methods from the tissue specimens from which the profiles or images have been generated and the protein markers to be identified have been detected. After protein extraction, we and others have generally chosen to utilize standard HPLC-based approaches for protein isolation using either ionic exchange and/or reverse-phase columns.[7,39,43−45,49] Each resulting fraction can then be mass-analyzed by MALDI−MS and/or high mass accuracy electrospray instruments such as QqTOF geometry mass spectrometers. The key points are that the protein is isolated in appreciable quantity (usually ∼1 mg) and that no reduction or alkylation steps are performed, therefore, minimizing the potential for changing its MW. In addition, one must carry out each step as quickly as possible, on ice when possible, and using degassed solvents in order to maintain protein integrity.

Several protein fractionation strategies revolve around a size-based separation (1D PAGE or size exclusion chromatography) combined with reverse-phase LC-MALDI−MS. The size-based approach can be carried out either before (followed by electroelution in the case of the 1D PAGE) or after the LC-MALDI step. The LC-MALDI−MS approach can be carried out very simply and quickly with the aid of robotics such as MALDI plate spotters. With the advent of LC-MALDI spotters (such as the Accuspot, Shimadzu Scientific Instruments, Columbia, MD), this approach can be streamlined to a great extent with high-throughput MALDI instruments that now work at repetition rates of 200 Hz, which are complemented by software packages that process and visualize the output files automatically (such as, for example, the WARP-LC software, Bruker Daltonics). Automated data analysis routines streamline this type of an approach, transforming many days of work into hours.

One such automated approach to protein identification includes either a 1D (RF) or 2D strong cation exchange/reversed-phase (SCX/RP) HPLC separation strategy and a 1D PAGE step that is complemented by either in-gel digestion or passive elution (followed by MALDI−MS on the parent ion and digestion). Figure 8 presents an example of such an experiment. After separation by HPLC of a tissue lysate, the resulting fractions were automatically analyzed by MALDI−MS. Figure 8a depicts the output of the MALDI−MS run displaying over 3000 distinct protein signals. Each fraction was then quantified for protein content using the EZQuant kit (Carlsbad, CA) (Figure 8b), and run on a 17% tricine 1D PAGE gel, which was visualized using colloidal coomassie and an IR scanner (LI-COR Biotechnology, Lincoln, NE) (Figure 8c). This is a quick and inexpensive way to visualize low MW proteins with high dynamic range and sensitivity, close to that of fluorescent dyes. For each HPLC fraction, correlations can then be made between the proteins signals detected in the MALDI−MS run and the various gel bands. The main limitations associated with 1D gel approaches relate to the low sensitivity in staining low molecular weight peptides and proteins, combined with difficulty in predicting the appropriate MW by migration alone. However, gels are ideal to detect coeluting higher molecular weight proteins not necessarily observed in the MALDI mass spectra, but easily observed in a 1D gel. To determine which gel bands correspond to the targeted protein biomarkers,

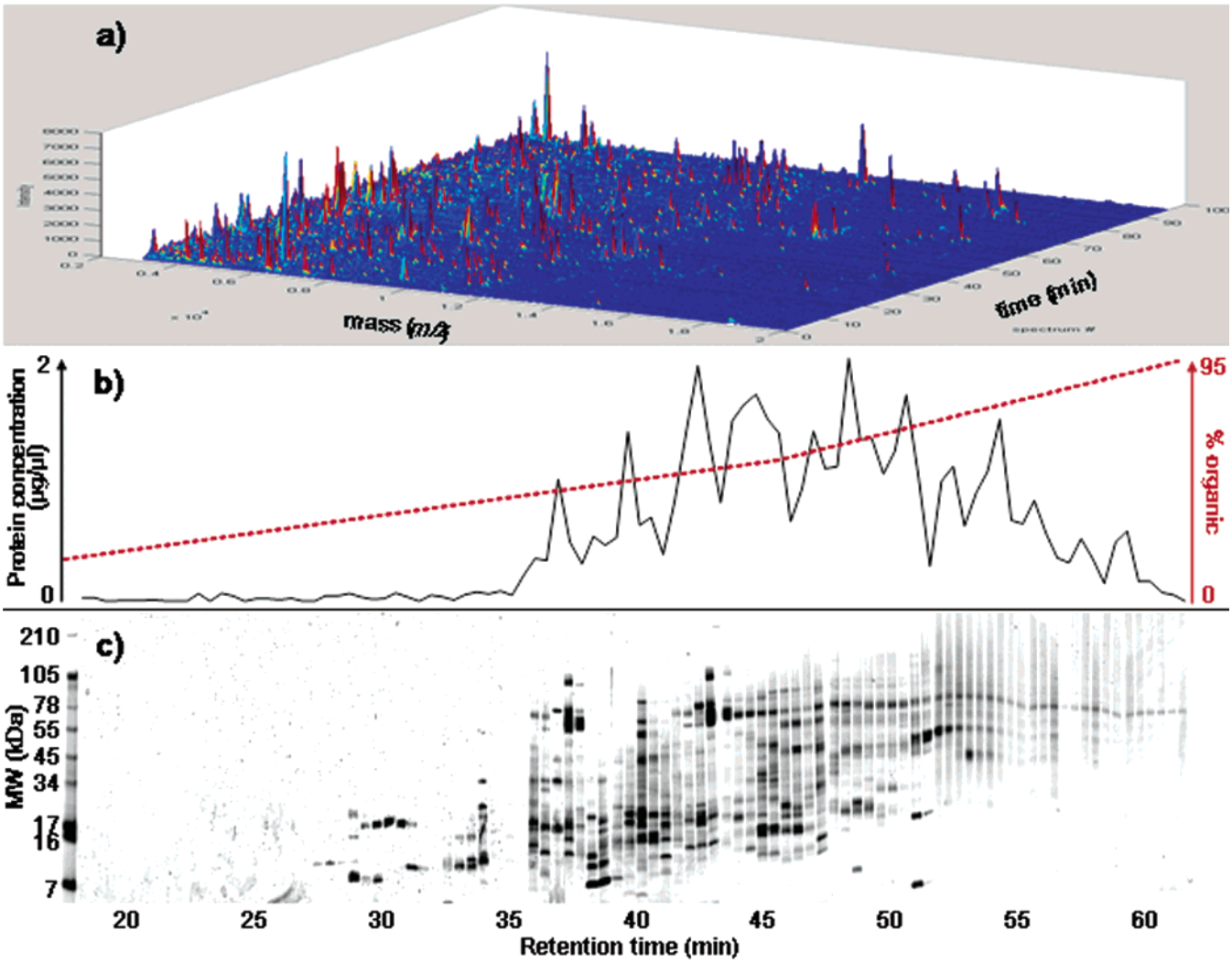

Figure 8. Protein isolation strategy toward high-throughput protein identification. A tissue protein extract is fractionated by RP-HPLC. (a) Output of the LC-MALDI−MS run, which displays >3000 peaks. (b) Each HPLC fraction was quantified for protein content and (c) run on a 17% tricine 1D-PAGE gel stained with colloidal coomassie.

passive elution is carried out, followed by MALDI−MS measurements to confirm the MWs. Automated spot picking and trypsin digestion is then performed, followed by peptide mapping and sequencing by MALDI−MS and MS/MS in high-throughput mode, which greatly streamlines the whole protein identification process. We have used this type of strategy to identify as many as 100 proteins in a single week with high, albeit not absolute, confidence. In addition, pooled disease and normal samples may be run in parallel to more closely match proteins of similar MWs using normalized intensities for each fraction.

Concluding Remarks

Profiling and imaging mass spectrometry are rapidly becoming tools of interest to probe the molecular and, more specifically, the proteomic content of tissue specimens. Thin sections from these specimens can be cut and analyzed in order to assess the regional concentration of the observed molecular species in a completely unbiased way. This information can then be directly correlated to tissue histology. IMS can therefore be used as a discovery tool to understand molecular regionalization and expression in both healthy and diseased biopsies. One clear foreseen potential of this technology is playing a major role in patient diagnosis and prognosis. This is especially true for cancers where, diagnosis and prognosis can be predicted based on the detection of key proteins from needle or resected biopsies. In a broader context for a patient, molecular information obtained from IMS and other sources is foreseen to be important in establishing a personalized therapy tailored to fight the disease with maximum efficiency.[15]

As currently performed, IMS is particularly well-adapted for the study of peptides proteins in a MW range up to ~30 000. Protocols and instrumentation to accurately investigate higher MW proteins from tissue sections are clearly needed. Further, most established protocols are only efficient in analyzing soluble proteins. Membrane-bound or associated hydrophobic proteins are not analyzed because the solvent systems used for MALDI are not efficient in disrupting lipid bylayers to solubilize these. The recent developments of new classes of degradable and MALDI-compatible surfactants[58−60] should open the door toward the developments of methodologies to analyze hydrophobic proteins directly from tissue sections. Overall, from a single analysis, one would like to be able to detect not only hundreds but thousands of different protein

species, and any development in instrumentation or tissue processing and matrix deposition protocols that promote this aspect should be encouraged.

All of the methodologies developed to date for protein analysis by IMS have been optimized from freshly frozen tissue specimens. Snap-freezing of tissue sample is ideal from a protein stand point, because no processing is involved and, when performed rapidly, avoids protein degradation through proteolysis. Transposed in a clinical setting, the processing of biopsies to be analyzed by IMS for diagnostic purposes needs to be very systematic and well-organized. Historically, biopsy samples analyzed in most pathology laboratories undergo formalin fixation, dehydration through graded alcohol series, and paraffin embedding (formaldehyde-fixed paraffin-embedded, FFPE). Although histology is, in this case, of improved quality with respect to freshly frozen samples, the molecular cross-linking by formaldehyde renders genomic and proteomic analysis difficult. However, tissue banks around the world contain literally millions of such specimens archived over decades for some of which excellent patient histories have been collected. Therefore, these FFPE samples hold enormous potential, and methodologies to quarry these by IMS need to be developed.

Although hundreds of different peptides and proteins can be imaged in a matter of hours and tens of tissue biopsies investigated in a day, the rigorous identification, characterization, and validation of these still takes a significant amount of time. Streamlining protein isolation and identification in a reproducible and automated fashion are important aspects to develop. Validating protein identification is also a very important part of the identification process. In most instances, the MWs observed for proteins are influenced by post-translational events, such as sequence deletions, and addition of chemical groups, such as phosphorylation or glycosylation events. The MW of the database entry may not reflect these secondary processes and will vary with respect to the MW observed. Validation of protein identification may be performed in several ways, including immunohistochemistry and immunoprecipitation followed by MS measurement of the precipitated product. In parallel, the development of mass spectrometry instrumentation and methodologies for top-down protein identification enabling the successful and meaningful fragmentation of singly charged higher MW protein species directly generated and detected off of tissue sections would literally revolutionize the way proteins are identified.

Acknowledgment. The authors thank Jeff Marks (Duke University) for providing the breast tumor biopsies, Hans Rudolf Aerni (Vanderbilt University) for his help in generating the data presented in Figure 4, Thao Dang (Vanderbilt University) for providing the xenograft, and Martha Guix (Vanderbilt University) for her help in generating the data presented in Figure 8. The authors also acknowledge support from the NIH (GM 58008-08), and NCI (CA 86243-03 and CA 116123-01).

References

(1) Pacholski, M. L.; Winograd, N. Imaging with mass spectrometry. *Chem. Rev.* **1999**, *99*, 2977−3005.
(2) Todd, P. J.; Schhaaff, T. G.; Chaurand, P.; Caprioli, R. M. Organic ion imaging of biological tissue with SIMS and MALDI. *J. Mass Spectrom.* **2001**, *36* (4), 355−369.
(3) McDonnell, L. A.; Piersma, S. R.; Altelaar, A. F. M.; Mize, T. H.; Luxembourg, S. L.; Verhaert, P.; van Minnen, J.; Heeren, R. M. A. Subcellular imaging mass spectrometry of brain tissue. *J. Mass Spectrom.* **2005**, *40* (2), 160−168.
(4) Brunelle, A.; Touboul, D.; Laprevote, O. Biological tissue imaging with time-of-flight secondary ion mass spectrometry and cluster ion sources. *J. Mass Spectrom.* **2005**, *40* (8), 985−999.
(5) Jackson, S. N.; Wang, H. Y. J.; Woods, A. S. Direct profiling of lipid distribution in brain tissue using MALDI-TOFMS. *Anal. Chem.* **2005**, *77* (14), 4523−4527.
(6) Wiseman, J. M.; Puolitaival, S. M.; Takats, Z.; Cooks, R. G.; Caprioli, R. M. Mass spectrometric profiling of intact biological tissue by using desorption electrospray ionization. *Angew. Chem., Int. Ed.* **2005**, *44* (43), 7094−7097.
(7) Stoeckli, M.; Chaurand, P.; Hallahan, D. E.; Caprioli, R. M. Imaging mass spectrometry: A new technology for the analysis of protein expression in mammalian tissues. *Nat. Med.* **2001**, *7* (4), 493−496.
(8) Chaurand, P.; Schwartz, S. A.; Caprioli, R. M. Profiling and imaging proteins in tissue sections by mass spectrometry. *Anal. Chem.* **2004**, *76* (5), 86A−93A.
(9) Chaurand, P.; Caprioli, R. M. Direct profiling and imaging of peptides and proteins from mammalian cells and tissue sections by mass spectrometry. *Electrophoresis* **2002**, *23* (18), 3125−3135.
(10) Aerni, H. R.; Cornett, D. S.; Caprioli, R. M. Automated acoustic matrix deposition for MALDI sample preparation. *Anal. Chem* **2006**, *78* (3), 827−834.
(11) Schwartz, S. A.; Reyzer, M. L.; Caprioli, R. M. Direct tissue analysis using matrix-assisted laser desorption/ionization mass spectrometry: practical aspects of sample preparation. *J. Mass Spectrom.* **2003**, *38* 699−708.
(12) Stoeckli, M.; Farmer, T. B.; Caprioli, R. M. Automated mass spectrometry imaging with a matrix-assisted laser desorption ionization time-of-flight instrument. *J. Am. Soc. Mass Spectrom.* **1999**, *10* (1), 67−71.
(13) Stoeckli, M.; Staab, D.; Staufenbiel, M.; Wiederhold, K.-H.; Signor, L. Molecular imaging of amyloid beta peptides in mouse brain sections using mass spectrometry. *Anal. Biochem.* **2002**, *311* (1), 33−39.
(14) Chaurand, P.; Sanders, M. E.; Jensen, R. A.; Caprioli, R. M. Proteomics in diagnostic pathology: Profiling and imaging proteins directly in tissue sections. *Am. J. Pathol.* **2004**, *165* (4), 1057−1068.
(15) Caprioli, R. M. Deciphering protein molecular signatures in cancer tissues to aid in diagnosis, prognosis, and therapy. *Cancer Res.* **2005**, *65* (23), 10642−10645.
(16) Troendle, F. J.; Reddick, C. D.; Yost, R. A. Detection of pharmaceutical compounds in tissue by matrix- assisted laser desorption/ionization and laser desorption/chemical ionization tandem mass spectrometry with a quadrupole ion trap. *J. Am. Soc. Mass Spectrom.* **1999**, *10* (12), 1315−1321.
(17) Reyzer, M. L.; Hsieh, Y.; Ng, K.; Korfmacher, W. A.; Caprioli, R. M. Direct analysis of drug candidates in tissue by matrix-assisted laser desorption/ionization mass spectrometry. *J. Mass Spectrom.* **2003**, *38* (10), 1081−1092.
(18) Wang, H. Y. J.; Jackson, S. N.; McEuen, J.; Woods, A. S. Localization and analyses of small drug molecules in rat brain tissue sections. *Anal. Chem.* **2005**, *77* (20), 6682−6686.
(19) Reyzer, M. L.; Caldwell, R. L.; Dugger, T. C.; Forbes, J. T.; Ritter, C. A.; Guix, M.; Arteaga, C. L.; Caprioli, R. M. Early changes in protein expression detected by mass spectrometry predict tumor response to molecular therapeutics. *Cancer Res.* 2**004**, *64*, (24), 9093−9100.
(20) Reyzer, M. L.; Caprioli, R. M. MALDI mass spectrometry for direct tissue analysis: A new tool for biomarker discovery. *J. Proteome Res.* **2005**, *4* (4), 1138−1142.
(21) Chaurand, P.; Schwartz, S. A.; Billheimer, D.; Xu, B. J.; Crecelius, A.; Caprioli, R. M. Integrating histology and imaging mass spectrometry. *Anal. Chem.* **2004**, *76* (4), 1145−1155.
(22) Caldwell, R. L.; Caprioli, R. M. Tissue profiling by mass spectrometry−A review of methodology and applications. *Mol. Cell. Proteomics* **2005**, *4* (4), 394−401.
(23) Tempez, A.; Ugarov, M.; Egan, T.; Schultz, J. A.; Novikov, A.; Della-Negra, S.; Lebeyec, Y.; Pautrat, M.; Caroff, M.; Smentkowski, V. S.; Wang, H. Y. J.; Jackson, S. N.; Woods, A. S. Matrix implanted laser desorption ionization (MILDI) combined with ion mobility-mass spectrometry for bio-surface analysis. *J. Proteome Rese.* **2005**, *4* (2), 540−545.
(24) Lemaire, R.; Tabet, J. C.; Ducoroy, P.; Hendra, J. B.; Salzet, M.; Fournier, I. Solid ionic matrixes for direct tissue analysis and MALDI imaging. *Anal. Chem.* **2006**, *78* (3), 809−819.

(25) Spengler, B.; Hubert, M. Scanning microprobe matrix-assisted laser desorption ionization (SMALDI) mass spectrometry: Instrumentation for sub-micrometer resolved LDI and MALDI surface analysis. *J. Am. Soc. Mass Spectrom.* **2002**, *13* (6), 735−748.
(26) Luxembourg, S. L.; Mize, T. H.; McDonnell, L. A.; Heeren, R. M. A. High-spatial resolution mass spectrometric imaging of peptide and protein distributions on a surface. *Anal. Chem.* **2004**, *76* (18), 5339−5344.
(27) Luxembourg, S. L.; McDonnell, L. A.; Mize, T. H.; Heeren, R. M. A. Infrared mass spectrometric imaging below the diffraction limit. *J. Proteome Res.* **2005**, *4* (3), 671−673.
(28) Altelaar, A. F. M.; van Minnen, J.; Jimenez, C. R.; Heeren, R. M. A.; Piersma, S. R. Direct molecular Imaging of *Lymnaea stagnalis* nervous tissue at subcellular spatial resolution by mass spectrometry. *Anal. Chem.* **2005**, *77* (3), 735−741.
(29) Jurchen, J. C.; Rubakhin, S. S.; Sweedler, J. V. MALDI-MS imaging of features smaller than the size of the laser beam. *J. Am. Soc. Mass Spectrom.* **2005**, *16* (10), 1654−1659.
(30) Crecelius, A. C.; Cornett, D. S.; Caprioli, R. M.; Williams, B.; Dawant, B. M.; Bodenheimer, B. Three-dimensional visualization of protein expression in mouse brain structures using imaging mass spectrometry. *J. Am. Soc. Mass Spectrom.* **2005**, *16* (7), 1093−1099.
(31) McCombie, G.; Staab, D.; Stoeckli, M.; Knochenmuss, R. Spatial and spectral correlations in MALDI mass spectrometry images by clustering and multivariate analysis. *Anal. Chem.* **2005**, *77* (19), 6118−6124.
(32) Sugiura, Y.; Shimma, S.; Setou, M. Thin sectioning improves the peak intensity and signal-to-noise ratio in direct tissue mass spectrometry. *J. Mass Spectrom. Soc. Jpn.* **2006**, *54* (2), 45−48.
(33) Xu, B. J.; Caprioli, R. M.; Sanders, M. E.; Jensen, R. A. Direct analysis of laser capture microdissected cells by MALDI mass spectrometry. *J. Am. Soc. Mass Spectrom.* **2002**, *13*, 1292−1297.
(34) Holle, A.; Haase, A.; Kayser, M.; Höhndorf, J. Optimizing UV laser focus profiles for improved MALDI performance. *J. Mass Spectrom.* **2006**, *41* (6), 705−716.
(35) Cornett, D. S.; Andersson, M.; Caprioli, R. M. In *An Automated Workflow for Improving the Speed and Specificity of Tissue Profiling*, 53rd ASMS Conference on Mass Spectrometry and Allied Topics, San Antonio, TX, 2005.
(36) Rohner, T. C.; Staab, D.; Stoeckli, M. MALDI mass spectrometric imaging of biological tissue sections. *Mech. Ageing Dev.* **2005**, *126* (1), 177−185.
(37) Crossman, L.; McHugh, N. A.; Hsieh, Y. S.; Korfmacher, W. A.; Chen, J. W. Investigation of the profiling depth in matrix-assisted laser desorption/ionization imaging mass spectrometry. *Rapid Commun. Mass Spectrom.* **2006**, *20* (2), 284−290.
(38) Chaurand, P.; Schwartz, S. A.; Caprioli, R. M. Imaging mass spectrometry: A new tool to investigate the spatial organization of peptides and proteins in mammalian tissue sections. *Curr. Opin. Chem. Biol.* **2002**, *6* (5), 676−681.
(39) Chaurand, P.; Fouchecourt, S.; DaGue, B. B.; Xu, B. J.; Reyzer, M. L.; Orgebin-Crist, M. C.; Caprioli, R. M. Profiling and imaging proteins in the mouse epididymis by imaging mass spectrometry. *Proteomics* **2003**, *3* 2221−2239.
(40) Kruse, R.; Sweedler, J. V. Spatial profiling invertebrate ganglia using MALDI MS. *J. Am. Soc. Mass Spectrom.* **2003**, *14* (7), 752−759.
(41) Chaurand, P.; Schwartz, S. A.; Caprioli, R. M. Assessing protein patterns in disease using imaging mass spectrometry. *J. Proteome Res.* **2004**, *3* (2), 245−252.
(42) Schwartz, S. A.; Weil, R. J.; Johnson, M. D.; Toms, S. A.; Caprioli, R. M. Protein profiling in brain tumors using mass spectrometry: Feasibility of a new technique for the analysis of protein expression. *Clin. Cancer Res.* **2004**, *10* (3), 981−987.
(43) Xie, L.; Xu, B. G. J.; Gorska, A. E.; Shyr, Y.; Schwartz, S. A.; Cheng, N.; Levy, S.; Bierie, B.; Caprioli, R. M.; Moses, H. L. Genomic and proteomic analysis of mammary tumors arising in transgenic mice. *J. Proteome Res.* **2005**, *4* (6), 2088−2098.
(44) Schwartz, S. A.; Weil, R. J.; Thompson, R. C.; Shyr, Y.; Moore, J. H.; Toms, S. A.; Johnson, M. D.; Caprioli, R. M. Proteomic-based prognosis of brain tumor patients using direct-tissue matrix-assisted laser desorption ionization mass spectrometry. *Cancer Res.* **2005**, *65* (17), 7674−7681.
(45) Yanagisawa, K.; Shyr, Y.; Xu, B. J.; Massion, P. P.; Larsen, P. H.; White, B. C.; Roberts, J. R.; Edgerton, M.; Gonzalez, A.; Nadaf, S.; Moore, J. H.; Caprioli, R. M.; Carbone, D. P. Proteomic patterns of tumour subsets in non-small-cell lung cancer. *Lancet* **2003**, *362* (9382), 433−439.
(46) Meistermann, H.; Norris, J. L.; Aerni, H.-R.; Cornett, D. S.; Friedlein, A.; Augustin, A.; de Vera Mudry, M. C.; Ruepp, S.; Suter, L.; Langen, H.; Caprioli, R. M.; Ducret, A. Biomarker identification by imaging mass spectrometry: Transthyretin is a biomarker for gentamicin-induced nephrotoxicity in rat. *Mol Cell. Proteomics* **2006**, in press.
(47) Brunelle, A.; Touboul, D.; Piednoel, H.; Voisin, V.; De La Porte, S.; Tallarek, E.; Hagenhoff, B.; Halgand, F.; Laprevote, O. Direct mapping on muscle tissues of duchenne myopathy biomarkers using both MALDI and cluster-SIMS imaging mass spectrometry. *Mol. Biol. Cell* **2004**, *15*, 103A−104A.
(48) Pierson, J.; Norris, J. L.; Aerni, H. R.; Svenningsson, P.; Caprioli, R. M.; Andren, P. E. Molecular profiling of experimental Parkinson's disease: Direct analysis of peptides and proteins on brain tissue sections by MALDI mass spectrometry. *J. Proteome Res.* **2004**, *3* (2), 289−295.
(49) Xu, B. J.; Shyr, Y.; Liang, X.; Ma, L. J.; Donnert, E. M.; Roberts, J. D.; Zhang, X.; Kon, V.; Brown, N. J.; Caprioli, R. M.; Fogo, A. B. Proteomic patterns and prediction of glomerulosclerosis and its mechanisms. *J. Am. Soc. Nephrol.* **2005**, *16* (10), 2967−2975.
(50) Laurent, C.; Levinson, D. F.; Schwartz, S. A.; Harrington, P. B.; Markey, S. P.; Caprioli, R. M.; Levitt, P. Direct profiling of the cerebellum by matrix-assisted laser desorption/ionization time-of-flight mass spectrometry: A methodological study in postnatal and adult mouse. *J. Neurosci. Res.* **2005**, *81* (5), 613−621.
(51) Pierson, J.; Svenningsson, P.; Caprioli, R. M.; Andren, P. E. Increased levels of ubiquitin in the 6-OHDA-lesioned striatum of rats. *J. Proteome Res.* **2005**, *4* (2), 223−226.
(52) Heinrich, R.; Gregorieva, J.; Tsypin, M. The use of mass spectra for cancer biomarker detection. http://www.efeckta.com/documents/MarkerWhitePaper.pdf (February 15, 2006).
(53) Norris, J. L.; Cornett, D. S.; Mobley, J. A.; Schwartz, S. A.; Roder, H.; Caprioli, R. M. In *Preparing MALDI Mass Spectra for Statistical Analysis: A Practical Approach*, 53nd ASMS Conference on Mass Spectrometry and Allied Topics, San Antonio, TX, 2005.
(54) Mobley, J. A.; Lam, Y. W.; Lau, K. M.; Pais, V. M.; L'Esperance, J. O.; Steadman, B.; Fuster, L. M. B.; Blute, R. D.; Taplin, M. E.; Ho, S. M. Monitoring the serological proteome: The latest modality in prostate cancer detection. *J. Urol.* **2004**, *172* (1), 331−337.
(55) Golub, T. R.; Slonim, D. K.; Tamayo, P.; Huard, C.; Gaasenbeek, M.; Mesirov, J. P.; Coller, H.; Loh, M. L.; Downing, J. R.; Caligiuri, M. A.; Bloomfield, C. D.; Lander, E. S. Molecular classification of cancer: Class discovery and class prediction by gene expression monitoring. *Science* **1999**, *286*, (5439), 531−537.
(56) Kirkpatrick, D. S.; Gerber, S. A.; Gygi, S. P. The absolute quantification strategy: A general procedure for the quantification of proteins and post-translational modifications. *Methods* **2005**, *35* (3), 265−273.
(57) Kutz, K. K.; Schmidt, J. J.; Li, L. J. In situ tissue analysis of neuropeptides by MALDI FTMS in-cell accumulation. *Anal. Chem.* **2004**, *76* (19), 5630−5640.
(58) Norris, J. L.; Porter, N. A.; Caprioli, R. M. Mass spectrometry of intracellular and membrane proteins using cleavable detergents. *Anal. Chem.* **2003**, *75* (23), 6642−6647.
(59) Norris, J. L.; Hangauer, M. J.; Porter, N. A.; Caprioli, R. M. Nonacid cleavable detergents applied to MALDI mass spectrometry profiling of whole cells. *J. Mass Spectrom.* **2005**, *40* (10), 1319−1326.
(60) Norris, J. L.; Porter, N. A.; Caprioli, R. M. Combination detergent/MALDI matrix: Functional cleavable detergents for mass spectrometry. *Anal. Chem.* **2005**, *77* (15), 5036−5040.
(61) Cornett, D. S.; Mobley, J. A.; Dias, E. C.; Andersson, M.; Arteaga, C. L.; Sanders, M. E.; Caprioli, R. M. A novel histology directed strategy for MALDI-MS tissue profiling that improves throughput and cellular specificity in human breast cancer. *Mol. Cell. Proteomics*, in press.

PR060346U